

# High-precision Wasserstein barycenters in polynomial time

Jason M. Altschuler

Enric Boix-Adserà

October 29, 2021

## Abstract

Computing Wasserstein barycenters is a fundamental geometric problem with widespread applications in machine learning, statistics, and computer graphics. However, it is unknown whether Wasserstein barycenters can be computed in polynomial time, either exactly or to high precision (i.e., with  $\text{polylog}(1/\varepsilon)$  runtime dependence). This paper answers these questions in the affirmative for any fixed dimension. Our approach is to solve an exponential-size linear programming formulation by efficiently implementing the corresponding separation oracle using techniques from computational geometry.

## 1 Introduction

Given discrete probability distributions  $\mu_1, \dots, \mu_k$  supported on  $\mathbb{R}^d$  and a vector  $\lambda \in \mathbb{R}^k$  of non-negative weights summing to 1, the corresponding *Wasserstein barycenters* are the probability distributions  $\nu$  minimizing

$$\operatorname{argmin}_{\nu} \sum_{i=1}^k \lambda_i \mathcal{W}(\mu_i, \nu), \quad (1.1)$$

where above  $\mathcal{W}(\cdot, \cdot)$  denotes the squared 2-Wasserstein distance [1]. Wasserstein barycenters provide a natural extension of the notion of averaging points to the notion of averaging point clouds. Importantly, they naturally inherit the ability of optimal transportation to capture geometric properties of the data. This desirable property has led to the widespread use of Wasserstein barycenters in many applications in statistics and machine learning [13, 17, 20, 23, 25], and in image processing and computer graphics [22, 24]; see also chapter 9.2 of the survey [21] and the references within.

However, despite considerable algorithmic work, it is an open problem (e.g., [8]) whether Wasserstein barycenters between discrete distributions can be exactly computed in polynomial time in the input size. A highly related open problem is whether Wasserstein barycenters can be computed to high accuracy, i.e., whether an  $\varepsilon$ -additively approximate solution for (1.1) can be computed in time that is polynomial in the input size and  $\log(1/\varepsilon)$ . This paper answers these questions in the affirmative for any fixed dimension  $d$ .

### 1.1 Prior work

The literature on computing Wasserstein barycenters is extensive and rapidly growing. While the Wasserstein barycenter problem can be formulated as a linear program (LP), a major obstacle is

---

The authors are with the Laboratory for Information and Decision Systems (LIDS), Massachusetts Institute of Technology, Cambridge MA 02139. Work partially supported by NSF Graduate Research Fellowship 1122374 and a Siebel scholarship.

that this LP has exponentially many variables, namely  $n^k$  where  $n$  denotes (an upper bound on) the support size of each  $\mu_i$  [3].<sup>1</sup> Existing algorithms with provable approximation guarantees work around this issue of exponential complexity by essentially assuming that some of the variables will be 0. Specifically, they restrict the support of the barycenter to a given set of points which is smaller than  $n^k$ , typically in one of the following two ways.

The most common “fixed support” approach restricts to an  $\varepsilon$ -grid in  $\mathbb{R}^d$ , which enables one to write the barycenter problem as an LP with roughly  $O(kn(R/\varepsilon)^d)$  variables, where  $R$  is a diameter bound on the supports of the input distributions. This new LP is tractable for standard LP solvers, or alternatively for specialized methods such as entropic regularization; see, e.g., [6, 10, 13, 19, 24, 26] among many others. However, this approach does not produce an exact barycenter, and in fact takes at least  $\text{poly}(n, k, (R/\varepsilon)^d)$  time to get an  $\varepsilon$ -additive approximation. In contrast, our proposed algorithm has polynomial dependence on  $\log(R/\varepsilon)$ .<sup>2</sup> In practice, this means that our algorithm can often solve up to machine precision, whereas previous methods can only provide limited accuracy—see §5 for experiments.

Another “fixed support” approach restricts to the union of the supports of the input distributions. While the resulting LP has  $O(nk)$  variables and thus can be solved in polynomial time, this method only gives a 2-multiplicative factor approximation [8].

## 1.2 Contribution

We give the first algorithm that, in any fixed dimension  $d$ , solves the Wasserstein barycenter problem exactly or to high precision in polynomial time. An overview of the algorithm is provided in §3. For simplicity of notation, throughout  $d$  is a constant; the running time for fixed  $d$  is  $(nk)^d$  times a polynomial in the input size.

**Theorem 1.1** (Computing high-precision barycenters). *There is an algorithm that, given  $k$  distributions each supported on  $n$  atoms in the ball of radius  $R$  in  $\mathbb{R}^d$ , a weight vector  $\lambda$ , and an accuracy  $\varepsilon > 0$ , computes an  $\varepsilon$ -additively approximate Wasserstein barycenter in  $\text{poly}(n, k, \log(R/\varepsilon))$  time. Moreover, the outputted barycenter has support size at most  $nk - k + 1$ .*

**Theorem 1.2** (Computing exact barycenters). *If the weight vector and distributions are represented with  $\log U$  bits of precision, then an exact barycenter can be found in  $\text{poly}(n, k, \log U)$  time. Moreover, the outputted barycenter has support size at most  $nk - k + 1$ .*

In addition to its polynomial runtime, our algorithm has two additional properties that may be useful in downstream applications. First, the outputted barycenter  $\nu$  has small support of  $O(nk)$  size, which is much smaller than the *a priori*  $n^k$  bound on the support size [3]. In particular, the support size of  $\nu$  is at most the maximal sparsity of any vertex of the transportation polytope between  $\mu_1, \dots, \mu_k$ —which is at most  $nk - k + 1$ . Note that Theorem 1.2 is not at odds with the NP-hardness of finding the sparsest barycenter [9]: indeed, our algorithm outputs a solution that albeit sparse is not necessarily the sparsest. Second, as a by-product, the algorithm also produces sparse solutions to the optimal transport problems  $\mathcal{W}(\mu_i, \nu)$  that are non-mass-splitting maps from  $\nu$  to  $\mu_i$ . Among other benefits, this enables easy visualization and interpretability of the results—in comparison to entropic-regularization based approaches which produce “blurry” dense maps. Details on both these points are in §3.

---

<sup>1</sup>We mention in passing that an orthogonal line of work aims to compute barycenters of *continuous* distributions (typically restricted to Gaussian distributions so that both  $\mu_i$  and  $\nu$  have compact representations for computational purposes); see, e.g., [2, 12] and the references within.

<sup>2</sup>Said equivalently, our algorithm is strongly polynomial, while previous algorithms are weakly polynomial.

Although the focus of this work is theoretical, we also provide preliminary numerical experiments in §5 demonstrating that when high-accuracy solutions are required, a slight variant of this algorithm can offer practical speed-ups over existing algorithms.

## 2 Notation

The set  $\{1, \dots, n\}$  is denoted by  $[n]$ . The  $k$ -fold product space  $\mathbb{R}^n \otimes \dots \otimes \mathbb{R}^n$  is denoted by  $(\mathbb{R}^n)^{\otimes k}$ , and similarly for  $(\mathbb{R}_{\geq 0}^n)^{\otimes k}$ . The  $j$ -th marginal,  $j \in [k]$ , of a tensor  $P \in (\mathbb{R}^n)^{\otimes k}$  is denoted by the vector  $m_j(P) \in \mathbb{R}^n$ , and has entries  $[m_j(P)]_i := \sum_{i_1, \dots, i_{j-1}, i_{j+1}, \dots, i_k} P_{i_1, \dots, i_{j-1}, i, i_{j+1}, \dots, i_k}$ . The transportation polytope between  $\mu_1, \dots, \mu_k$  is the set of joint distributions with one-dimensional marginal distributions  $\mu_1, \dots, \mu_k$ , and is identified with the set  $\mathcal{M}(\mu_1, \dots, \mu_k) := \{P \in (\mathbb{R}_{\geq 0}^n)^{\otimes k} : m_j(P) = \mu_j, \forall j \in [k]\}$ , where we abuse notation slightly by identifying  $\mu_i$  with its vector of probabilities (in any order). The closure of a set  $E \subset \mathbb{R}^d$  (with respect to the standard topology) is denoted by  $\overline{E}$ . Throughout, we assume without loss of generality that each  $\lambda_i$  is strictly positive, since otherwise  $\mu_i$  does not affect the barycenter (see (1.1)).

## 3 Algorithm overview

We describe the exact solver, as the approximate solver is implemented by exactly solving a rounded problem (see §4.3 for details). Our starting point is the known fact [3] that the barycenter  $\nu$  can be found by solving the multimarginal optimal transport problem

$$\min_{P \in \mathcal{M}(\mu_1, \dots, \mu_k)} \langle P, C \rangle, \quad (\text{MOT})$$

for the cost tensor  $C \in (\mathbb{R}^n)^{\otimes k}$  with entries

$$C_{j_1, \dots, j_k} = \min_{y \in \mathbb{R}^d} \sum_{i=1}^k \lambda_i \|x_{i, j_i} - y\|^2, \quad (3.1)$$

or equivalently,  $\sum_{i=1}^k \lambda_i \|x_{i, j_i} - \sum_{\ell=1}^k \lambda_{\ell} x_{\ell, j_{\ell}}\|^2$  by optimality of  $y = \sum_{\ell=1}^k \lambda_{\ell} x_{\ell, j_{\ell}}$ .

Specifically, if  $P$  is an optimal solution for (MOT) and the random variable  $X = (X_1, \dots, X_k)$  has law  $P$ , then the induced law of  $Y = \sum_{i=1}^k \lambda_i X_i$  is an optimal barycenter  $\nu$ . Furthermore, the support size of  $\nu$  is at most the support size of  $P$ , and also the coupling  $(Y, X_i)$  is a non-mass-splitting map that solves the optimal transport problem from  $\nu$  to  $\mu_i$ .<sup>3</sup>

However, solving this LP (MOT) presents a computational obstacle since it has  $n^k$  decision variables. Moreover, we desire a sparse solution  $P$ —rather than a generic solution which has exponentially many non-zero entries—since a polynomial sparsity for  $P$  ensures a polynomial support size for the final barycenter  $\nu$ . We describe below how to solve these issues in polynomial time.

**Step 1: reduction to separation oracle** It is a classical fact that regardless of the number of constraints, an LP with polynomially many variables can be solved in polynomial time so long as the corresponding separation oracle can be implemented in polynomial time (see, e.g., [7, §8.5]). While (MOT) is not such an LP since it has exponentially many variables, this result applies to its

---

<sup>3</sup>This is shown for the case of uniform weights  $\lambda_i = 1/k$  in [3]; it is a straightforward extension to show that this also holds for general weights.

dual

$$\max_{p_1, \dots, p_k \in \mathbb{R}^n} \sum_{i=1}^k \langle p_i, \mu_i \rangle \quad \text{subject to} \quad C_{j_1, \dots, j_k} - \sum_{i=1}^k [p_i]_{j_i} \geq 0, \quad \forall (j_1, \dots, j_k) \in [n]^k \quad (\text{MOT-D})$$

That is, we can efficiently solve (MOT-D) so long as we can efficiently implement the corresponding separation oracle, defined as follows.

**Definition 3.1** (Separation oracle for (MOT-D)). *Given  $p = (p_1, \dots, p_k) \in \mathbb{R}^{n \times k}$ , the oracle  $\text{SEP}$  returns a tuple  $\text{SEP}(p) \in \operatorname{argmin}_{(j_1, \dots, j_k) \in [n]^k} C_{j_1, \dots, j_k} - \sum_{i=1}^k [p_i]_{j_i}$ .*

To recover a primal solution requires additional work: while in general a dual solution does not necessarily “help” to find a primal solution [7, Exercise 4.17], we leverage the specific structure of the LP (MOT) to recover a primal solution from a dual solution in polynomial time. Formally, in §4.1 we show the following proposition. Note that it applies to general costs beyond just (3.1).

**Proposition 3.2.** *Let  $C \in (\mathbb{R}^n)^{\otimes k}$  be an arbitrary cost and let  $\log U$  be the maximum number of bits of precision in an entry of  $C$ . A vertex solution  $P^*$  for (MOT) can be found in  $\text{poly}(n, k, \log U)$  time and  $\text{poly}(n, k, \log U)$  calls to the oracle  $\text{SEP}$ .*

Proofs and further details for this step are provided in §4.1.

**Step 2: efficient algorithm for the separation oracle** In §4.2, we present a polynomial-time algorithm that implements the  $\text{SEP}$  oracle for the cost  $C$  in (3.1). To describe this algorithm, recall that this  $\text{SEP}$  oracle requires computing an optimal tuple for

$$\operatorname{argmin}_{(j_1, \dots, j_k) \in [n]^k} \min_{y \in \mathbb{R}^d} \sum_{i=1}^k \lambda_i (\|x_{i,j_i} - y\|^2 - [w_i]_{j_i}), \quad (3.2)$$

where above  $w_i$  denotes  $p_i/\lambda_i$ . At a high-level, our approach is to swap the order of minimization, optimize over  $y \in \mathbb{R}^d$ , and then (easily) recover an optimal tuple from this optimal  $y$ . The difficulty is in the optimization over  $y \in \mathbb{R}^d$ . The key to performing this efficiently is partitioning the space  $\mathbb{R}^d$  into a “cell complex” such that (i) the optimization over  $y$  in each cell is easy, and (ii) there are only polynomially many cells. Operationally, this allows us to reduce the separation oracle optimization (3.2) to optimizing over only a polynomially sized set of candidate tuples in  $[n]^k$ —one for each cell—which we moreover show can be efficiently identified and enumerated.

To formalize this, we make the following key definitions. Define for each  $i \in [k]$  and  $j \in [n]$  the set

$$E_{i,j} = \{y \in \mathbb{R}^d : \|x_{i,j} - y\|^2 - [w_i]_j < \|x_{i,j'} - y\|^2 - [w_i]_{j'}, \forall j' \neq j\}, \quad (3.3)$$

and define for each tuple  $(j_1, \dots, j_k) \in [n]^k$  the set

$$F_{j_1, \dots, j_k} = \bigcap_{i=1}^k E_{i,j_i}. \quad (3.4)$$

Geometrically, for each  $i \in [k]$ , the cells  $\{E_{i,j}\}_{j \in [n]}$  form a power diagram (defined in §4.2.2) that “essentially” partitions  $\mathbb{R}^d$  in the sense that these cells are disjoint and their closures cover  $\mathbb{R}^d$ ; see Figure 1 for an illustration. The cell complex  $\{F_{j_1, \dots, j_k}\}_{(j_1, \dots, j_k) \in [n]^k}$  is the intersection of these  $k$  power diagrams and “essentially” partitions  $\mathbb{R}^d$  in the analogous way; see Figure 2 for an illustration.

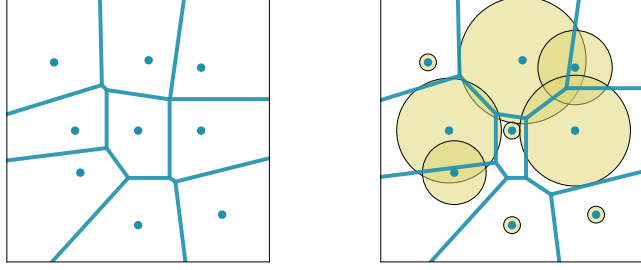


**Figure 1:** Two power diagrams on the same  $n = 9$  points with varying weights  $w$ . In the left diagram, all weights are zero, so it is a Voronoi diagram. In the right diagram, the weight of a point is indicated by the size of the ball around it. Increasing the weight of a point increases the size of its cell.

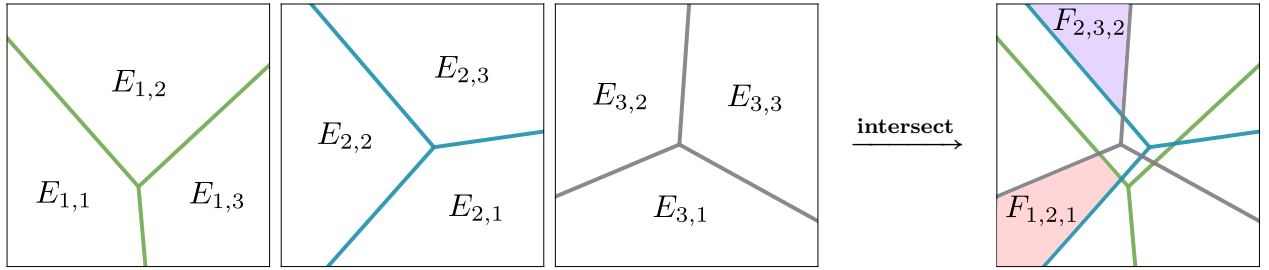


**Figure 2:** Illustrates  $k = 3$  power diagrams,  $\{\{E_{i,j}\}_{j \in [n]}\}_{i \in [k]}$  each with  $n = 3$  cells, and their intersection  $\{F_{j_1, \dots, j_k}\}_{(j_1, \dots, j_k) \in [n]^k}$ . For instance, the red cell in the intersected diagram is  $F_{1,2,1} = E_{1,1} \cap E_{2,2} \cap E_{3,1}$ , and the purple cell is  $F_{2,3,2} = E_{1,2} \cap E_{2,3} \cap E_{3,2}$ . Note that the intersected diagram has only 13 non-empty cells, which is less than  $n^k = 27$  (c.f., Lemma 3.4).

The heart of our algorithm lies in the following two lemmas. The first lemma shows that the optimization (3.2) over the exponentially many tuples in  $[n]^k$  may be restricted to just those whose corresponding cell  $F_{j_1, \dots, j_k}$  is non-empty, i.e., we may restrict to the tuples in

$$T := \{(j_1, \dots, j_k) \in [n]^k : F_{j_1, \dots, j_k} \neq \emptyset\}. \quad (3.5)$$

(This lemma also uses the closed-form expression for the optimal  $y$  for those tuples.) The second lemma shows that this candidate set  $T$  contains only polynomially many tuples and moreover can be efficiently enumerated.

**Lemma 3.3.** *The solution(s) to the separation oracle problem (3.2) are given by*

$$\operatorname{argmin}_{(j_1, \dots, j_k) \in T} \sum_{i=1}^k \lambda_i \|x_{i,j_i}\|^2 - \left\| \sum_{i=1}^k \lambda_i x_{i,j_i} \right\|^2 - \sum_{i=1}^k \lambda_i [w_i]_{j_i}. \quad (3.6)$$

**Lemma 3.4.** *The set  $T$  can be enumerated in  $\text{poly}(n, k, \log U)$  time in any fixed dimension  $d$ .*

The proofs of these two lemmas are presented respectively in §4.2.1 and §4.2.2. Briefly, the former exploits the fact that the optimization over  $y \in \mathbb{R}^d$  is equivalent to optimizing over the cells in  $F_{j_1, \dots, j_k}$ , and the latter exploits complexity bounds for the intersections of power diagrams.

Together, these two lemmas yield the desired efficient algorithm for the separation oracle.

**Proposition 3.5.** *If the cost  $C$  is given by (3.1), the oracle  $\text{SEP}(p)$  can be implemented in time  $\text{poly}(n, k, \log U)$ , where  $\log U$  is the number of bits of precision needed to represent the points  $x_{i,j} \in \mathbb{R}^d$ , weights  $\lambda_i \in \mathbb{R}_{>0}^k$  and potentials  $p \in \mathbb{R}^{n \times k}$ .*

*Proof.* Enumerate the set  $T$  using the algorithm in Lemma 3.4, and output a tuple in  $T$  minimizing (3.6). Correctness follows by Lemma 3.3.  $\square$

Combining Propositions 3.2 and 3.5 proves Theorem 1.1 aside from checking bit-complexity details, which is done formally in §4.3.

## 4 Algorithm details and proofs

### 4.1 Reduction to separation oracle (proof of Proposition 3.2)

We make use of the following runtime guarantee of the Ellipsoid algorithm, first proved by [18].

**Theorem 4.1** (Theorem 8.5 in [7]). *Let  $\log U$  be an upper bound on the number of bits needed to represent any entry in  $A \in \mathbb{R}^{M \times N}$ ,  $b \in \mathbb{R}^M$ , or  $c \in \mathbb{R}^N$ . Then the Ellipsoid algorithm solves  $\operatorname{argmin}\{c^T x : Ax \leq b, x \in \mathbb{R}^N\}$  in  $\operatorname{poly}(N, \log U)$  time and  $\operatorname{poly}(N, \log U)$  calls to a separation oracle for the polytope  $\{x : Ax \leq b\}$ .*

Since  $\text{SEP}(p)$  is a separation oracle for (MOT-D), Theorem 4.1 implies that an optimal solution for (MOT-D) can be found in  $\operatorname{poly}(N, \log U) = \operatorname{poly}(n, k, \log U)$  time. We now show how to use this to find an optimal solution  $P^*$  for (MOT).

Let  $L$  denote the number of  $\text{SEP}$  queries made by the Ellipsoid algorithm. For  $l \in [L]$ , let  $p^{(l)} \in \mathbb{R}^{n \times k}$  be the argument of the  $l$ -th query to  $\text{SEP}$ , and let  $j^{(l)} \in [n]^k$  be the returned tuple. Let  $S := \{j^{(l)}\}_{l=1}^L$  denote the set of all returned tuples, and let  $C'$  be the tensor that agrees with  $C$  on  $S$ , and equals  $2U$  elsewhere. For shorthand, let (MOT') denote the problem (MOT) where the cost  $C$  is replaced by  $C'$ . We make several observations.

**Lemma 4.2.** *The optimal values of (MOT) and (MOT') are equal.*

*Proof.* Since the Ellipsoid algorithm is deterministic and accesses the cost only through the  $\text{SEP}$  oracle, an inductive argument shows that all for all  $l \in [L]$ ,

$$\min_{(j_1, \dots, j_k) \in [n]^k} C'_{j_1, \dots, j_k} - \sum_{i=1}^k [p_i^{(l)}]_{j_i} = \min_{(j_1, \dots, j_k) \in [n]^k} C_{j_1, \dots, j_k} - \sum_{i=1}^k [p_i^{(l)}]_{j_i}.$$

That is,  $C'$  is consistent with  $C$  on the  $\text{SEP}$  queries made by the Ellipsoid algorithm. Therefore (MOT-D) has the same value with cost  $C'$  or  $C$ . We conclude by strong duality.  $\square$

**Lemma 4.3.** *Every optimal solution  $P^*$  for (MOT') is also an optimal solution for (MOT).*

*Proof.* By the entrywise inequality  $C \leq C'$ , we have  $\langle P^*, C \rangle \leq \langle P^*, C' \rangle$ . By Lemma 4.2, the latter equals the optimal value of (MOT). Thus  $P^*$  is optimal for (MOT).  $\square$

**Lemma 4.4.** *Every optimal solution for (MOT') is supported on  $S$ .*

*Proof.* If not, then there exists an optimal solution for (MOT') which has a different cost for (MOT) since  $C'$  is strictly larger than  $C$  on  $[n]^k \setminus S$ . But this solution is also optimal for (MOT) by Lemma 4.3, contradicting Lemma 4.2.  $\square$

We now conclude the proof of Proposition 3.2. By Lemmas 4.3 and 4.4, it suffices to solve (MOT') where we restrict the sparsity of  $P$  to the tuples in  $S$ . Since  $|S|$  is of size  $\operatorname{poly}(n, k, \log U)$  by Theorem 4.1, this is a polynomial size LP which can be solved in polynomial time with standard

LP solvers. Moreover, to ensure we obtain a vertex solution<sup>4</sup> while amplifying the final runtime by at most a polynomial factor, we can repeatedly remove tuples from  $S$  one at a time if the cost is unchanged with it removed.

## 4.2 Efficient algorithm for the separation oracle

### 4.2.1 Correctness (proof of Lemma 3.3)

For shorthand, denote a tuple  $(j_1, \dots, j_k) \in [n]^k$  by  $\vec{j}$ , and denote the objective function  $\sum_{i=1}^k \lambda_i(\|x_{i,j_i} - y\|^2 - [w_i]_{j_i})$  in the separation oracle optimization (3.2) by  $g(\vec{j}, y)$ .

We make use of the two following helper lemmas, which given either a tuple  $\vec{j}$  or a point  $y$ , explicitly solve for the other in the separation oracle's joint minimization  $\min_{\vec{j} \in [n]^k, y \in \mathbb{R}^d} g(\vec{j}, y)$ .

**Lemma 4.5.** *If  $y \in \overline{F_{\vec{j}}}$ , then  $\vec{j} \in \operatorname{argmin}_{\vec{\ell} \in [n]^k} g(\vec{\ell}, y)$ .*

*Proof.* By separability of  $g$  in the coordinates of  $\vec{\ell}$  and non-negativity of  $\lambda_i$ , for each  $i \in [n]$  the optimal  $\ell_i$  is a solution of  $\operatorname{argmin}_{\ell_i \in [n]} \|x_{i,\ell_i} - y\|^2 - [w_i]_{\ell_i}$ . But  $\overline{E_{i,j_i}}$  contains  $y$  by construction of  $F_{j_1, \dots, j_k}$  (see (3.4)), and thus  $j_i$  is a solution for this by definition of  $E_{i,j_i}$  (see (3.3)).  $\square$

**Lemma 4.6.** *If  $\vec{j} \in [n]^k$ , then  $\sum_{i=1}^k \lambda_i x_{i,j_i} \in \operatorname{argmin}_{y \in \mathbb{R}^d} g(\vec{j}, y)$ .*

*Proof.* Immediate from first-order optimality conditions.  $\square$

*Proof of Lemma 3.3.* We show the separation oracle optimization equals  $\min_{\vec{j} \in T} \min_{y \in \mathbb{R}^d} g(\vec{j}, y)$ :

$$\min_{\vec{j} \in T} \min_{y \in \mathbb{R}^d} g(\vec{j}, y) \geq \min_{y \in \mathbb{R}^d} \min_{\vec{\ell} \in [n]^k} g(\vec{\ell}, y) = \min_{\vec{j} \in T} \min_{y \in \overline{F_{\vec{j}}}} \min_{\vec{\ell} \in [n]^k} g(\vec{\ell}, y) = \min_{\vec{j} \in T} \min_{y \in \overline{F_{\vec{j}}}} g(\vec{j}, y) \geq \min_{\vec{j} \in T} \min_{y \in \mathbb{R}^d} g(\vec{j}, y).$$

Above, the first step is by restricting the optimization and swapping the order of minimizations, the second step is by the fact that  $\{\overline{F_{j_1, \dots, j_k}}\}_{(j_1, \dots, j_k) \in T}$  covers  $\mathbb{R}^d$ , the third step is by Lemma 4.5, and the last by restricting the optimization. Now by Lemma 4.5,

$$\min_{\vec{j} \in T} \min_{y \in \mathbb{R}^d} g(\vec{j}, y) = \min_{\vec{j} \in T} g(\vec{j}, \sum_{i=1}^k \lambda_i x_{i,j_i}).$$

Simplifying the objective concludes the proof.  $\square$

### 4.2.2 Runtime (proof of Lemma 3.4)

A key ingredient in the proof is power diagrams. As such, we first introduce these objects and some basic facts about their complexity. Although  $d$  is a fixed constant in our final results, we state the explicit dependence on the dimension  $d$  in these power diagram complexity bounds to highlight how and where our algorithm incurs exponential runtime dependence in  $d$ .

**Definition 4.7.** *The power diagram on the spheres  $S(z_1, r_1), \dots, S(z_n, r_n)$  with centers  $z_j \in \mathbb{R}^d$  and radii  $r_j \geq 0$  is the cell complex whose cells  $E_1, \dots, E_n$  are given by*

$$E_j = \{y \in \mathbb{R}^d : \|z_j - y\|^2 - r_j^2 < \|z_{j'} - y\|^2 - r_{j'}^2, \forall j' \neq j\}.$$

Note that for each  $i \in [k]$ , the sets  $\{E_{i,j}\}_{j \in [k]}$  defined in (3.3) form a power diagram on the spheres  $S(x_{i,1}, r_{i,1}), \dots, S(x_{i,n}, r_{i,n})$ , where the  $j$ -th sphere is centered at point  $x_{i,j}$  and has radius  $r_{i,j} := \sqrt{[w_i]_j - \min_{j'} [w_i]_{j'}}$ .

<sup>4</sup>In practice, this could be accomplished more simply by using the Simplex algorithm.

**Lemma 4.8** (Theorems 1 and 7 of [4], using convex hull algorithm of [11]). *A power diagram on  $n$  spheres in  $\mathbb{R}^d$  has  $O(n)$  affine facets of dimension  $d - 1$ . Moreover these facets can be computed in  $O((n \log n + n^{\lceil d/2 \rceil}) \cdot \text{polylog } U)$  time, where  $\log U$  is the number of bits of precision.*

**Lemma 4.9** (Theorem 3.3 of [15]). *The cell complex formed by an arrangement of  $N$  hyperplanes in  $\mathbb{R}^d$ , represented up to  $\log U$  bits of precision, can be computed in  $N^d \cdot \text{polylog}(NU)$  time.*

*Proof of Lemma 3.4.* In all running times here,  $d$  is a fixed constant. By Lemma 4.8, the  $O(nk)$  total facets for the  $k$  power diagrams  $\{\{E_{i,j}\}_{i \in [n]}\}_{j \in [k]}$  can be computed in  $\text{poly}(n, k, \log U)$  time. For each facet, compute the  $(d-1)$ -dimensional hyperplane it lies in. The cell complex  $\mathcal{H}$  formed by these hyperplanes is a subcomplex of the cell complex formed by intersecting the power diagrams. By Lemma 4.9, we can enumerate the cells in  $\mathcal{H}$  in  $\text{poly}(n, k, \log U)$  time. For each cell in  $\mathcal{H}$ , the corresponding tuple  $(j_1, \dots, j_k) \in [n]^k$  is computable in  $O(nk \cdot \text{polylog } U)$  time by computing the  $k$  coordinates of the tuple separately. Since each non-empty cell  $F_{j_1, \dots, j_k}$  contains at least one cell in  $\mathcal{H}$ , this process enumerates all tuples in  $T$ .  $\square$

### 4.3 Putting the pieces together

*Proof of Theorem 1.2.* Assume each  $x_{i,j_i}$  and  $\lambda_i$  is written to  $\log U$  bits of precision. Since each entry of the cost tensor (3.1) requires only  $O(\log k + \log U)$  bits of precision, and since the parameter  $w \in \mathbb{R}^{n \times k}$  in each SEP query made by the algorithm in Proposition 3.2 requires only  $\text{poly}(n, k, \log U)$  bits of precision, it follows that the algorithm in Proposition 3.2 combined with the SEP oracle implementation in Proposition 3.5 computes a vertex solution  $P^*$  for (MOT) in  $\text{poly}(n, k, \log U)$  time. Since (MOT) is a standard-form LP whose constraints have rank at most  $nk - k + 1$ , each vertex solution  $P^*$  has at most  $nk - k + 1$  non-zero entries. Thus we can recover from  $P^*$  an optimal barycenter  $\nu$  with support size at most  $nk - k + 1$  in time  $\text{poly}(n, k, \log U)$  by the reduction in §3.  $\square$

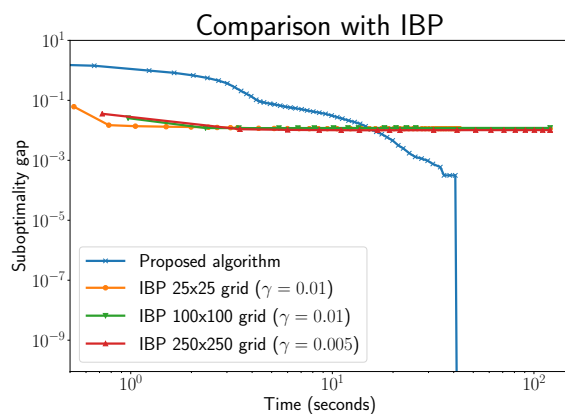
*Proof of Theorem 1.1.* By rounding both the weights  $\lambda_i$  and the coordinates of the atoms  $x_{i,j} \in \mathbb{R}^d$  to  $\text{poly}(\varepsilon/(Rkd))$  additive accuracy, it can be ensured that each of these numbers requires only  $O(\log(Rkd/\varepsilon))$  bits of precision and also that the objective function  $\nu \mapsto \sum_{i=1}^k \lambda_i \mathcal{W}(\mu_i, \nu)$  for the barycenter optimization (1.1) is preserved pointwise to  $\varepsilon$  additive accuracy. This follows from a straightforward calculation and the fact (immediate from the definition of optimal transportation [27, §1] and an application of Hölder's inequality) that if the squared Euclidean distance between each atom of  $\mu_i$  and each atom of  $\nu$  is preserved up to  $\varepsilon'$  additive accuracy, then the squared 2-Wasserstein distance  $\mathcal{W}(\mu_i, \nu)$  is preserved up to  $\varepsilon'$  additive accuracy. Now solve the barycenter problem for the rounded weights and atoms exactly using Theorem 1.2.  $\square$

## 5 Numerical implementation

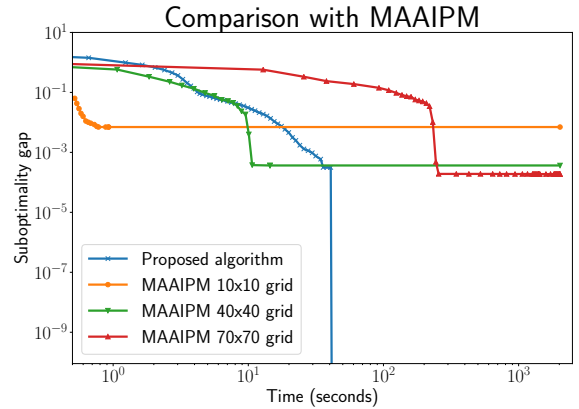
While the focus of this paper is theoretical, here we briefly mention that when high-precision solutions are desired, a slight variant of our algorithm can provide practical speedups over state-of-the-art algorithms. To demonstrate this, we implement our algorithm for dimension  $d = 2$  in Python. The only difference between our numerical implementation and the theoretical algorithm described above is that we use a standard cutting-plane method (see, e.g., [7, §6.3]) for the “outer loop” rather than the Ellipsoid algorithm due to its good practical performance. Code and further implementation details are provided on Github.<sup>5</sup>

Figure 3 demonstrates that our algorithm solves the barycenter problem (1.1) to machine precision on an instance with  $k = 10$  uniform distributions each on  $n = 20$  points randomly drawn

<sup>5</sup>[https://github.com/eboix/high\\_precision\\_barycenters](https://github.com/eboix/high_precision_barycenters)



(a) Comparison against the Iterated Bregman Projection (IBP) algorithm of [24] using their implementation <https://github.com/gpeyre/2015-SIGGRAPH-convolutional-ot>.



(b) Comparison against the Matrix-based Adaptive Alternating Interior-Point Method (MAAIPM) of [16] using their implementation <https://gitlab.com/ZXiong/wasserstein-barycenter>.

**Figure 3:** Comparison with state-of-the-art algorithms. The  $y$ -axis is the suboptimality for the barycenter optimization (1.1); note that while standard LP solvers cannot be run at this scale, our algorithm yields an exact solution (certified by our separation oracle) which enables plotting this suboptimality. Both compared algorithms require a fixed-support assumption and are run on uniform grids of increasing sizes. IBP has an additional parameter: the entropic regularization  $\gamma$ , which significantly impacts the algorithm’s accuracy and numerical stability. We provide a generous comparison here for IBP by (i) fine-tuning  $\gamma$  for it (we binary search for the most accurate  $\gamma$ ; note that their code does not always converge for  $\gamma$  small due to numerical instability); and (ii) exactly computing the Wasserstein distances  $\mathcal{W}(\mu_i, \nu)$  to IBP’s current barycenter  $\nu$  in the barycenter objective (1.1) using [14], which is more accurate than IBP’s approximation (this is slow for large grids but is not counted in IBP’s timing). Our algorithm finds an exact barycenter after  $\sim 50$  seconds. All experiments are run on a standard 2014 Lenovo Yoga 720-13IKB laptop.

from  $[-1, 1]^2 \subset \mathbb{R}^2$ . In contrast, existing popular barycenter algorithms which use the fixed-support assumption can converge faster but only to lower-precision approximations. This is because the  $\Theta(1/\varepsilon^d)$  gridsize that they require for  $\varepsilon$ -additive approximation results in a large-scale LP which is prohibitive even for relatively low precision  $\varepsilon$ ; see §1.1 for details. Note also that a standard LP solver requires optimizing over  $n^k = 20^{10} \approx 10^{13}$  variables for the LP formulation (MOT) and thus is clearly infeasible at this scale.

## 6 Discussion

Wasserstein barycenters are used in many applications despite the fact that fundamental questions about their computational complexity are open—in particular, it was previously unknown whether barycenters can be computed in polynomial time. This paper addresses this issue by giving the first algorithm that, in any fixed dimension  $d$ , solves the barycenter problem exactly or to high precision in polynomial time.

Now, while our result answers the polynomial-time computability of barycenters from a *theoretical* perspective, from a *practical* perspective it is still a hard and interesting problem to compute high-precision barycenters for large-scale inputs. Indeed, our current implementation is not efficient beyond moderate-scale inputs; and while existing algorithms such as IBP scale to larger inputs, they have limited accuracy. Moreover, all existing algorithms pay for the curse of dimensionality in

one way or another. We emphasize that our implementation does not contain further optimizations or heuristics; it is an interesting direction for future work to investigate potential such options including pruning cutting planes, warm starts, and specially tailored algorithms for the Voronoi intersections in §4.2.2 (e.g., in  $\mathbb{R}^2$  or  $\mathbb{R}^3$ , settings which commonly arise in image processing and computer graphics applications). Empirical studies on real-world datasets may also suggest further helpful heuristics.

We mention in passing that the techniques we develop in this paper readily extend to solving related problems such as polynomial-time algorithms for computing the geometric median of probability measures over  $\mathbb{R}^d$  with respect to the 1-Wasserstein metric  $\rho$  (a.k.a., Earth Mover’s Distance) over either the base metric  $\ell_1$  or  $\ell_\infty$ . This geometric median problem is defined as  $\inf_{\mu, \nu} \sum_{i=1}^k \lambda_i \rho(\mu_i, \nu)$  (see, e.g., [5]), and can be solved using our algorithm developed for Wasserstein barycenters so long as the corresponding separation oracle **SEP** still has a polynomial-time implementation. In the aforementioned cases where the base metric is  $\ell_1$  or  $\ell_\infty$ , the analogues of the power diagrams in our **SEP** oracle can still be expressed as cell complexes with polynomially many affine facets (in fixed dimension), and thus similar techniques yield polynomial-time algorithms.

## Acknowledgements.

We thank Sinho Chewi, Jonathan Niles-Weed, and Pablo Parrilo for helpful conversations.

## References

- [1] M. Aguech and G. Carlier. Barycenters in the Wasserstein space. *SIAM Journal on Mathematical Analysis*, 43(2):904–924, 2011.
- [2] P. C. Álvarez-Esteban, E. Del Barrio, J. Cuesta-Albertos, and C. Matrán. A fixed-point approach to barycenters in Wasserstein space. *Journal of Mathematical Analysis and Applications*, 441(2):744–762, 2016.
- [3] E. Anderes, S. Borgwardt, and J. Miller. Discrete Wasserstein barycenters: Optimal transport for discrete data. *Mathematical Methods of Operations Research*, 84(2):389–409, 2016.
- [4] F. Aurenhammer. Power diagrams: properties, algorithms and applications. *SIAM Journal on Computing*, 16(1):78–96, 1987.
- [5] M. Bacák. Computing medians and means in Hadamard spaces. *SIAM Journal on Optimization*, 24(3):1542–1566, 2014.
- [6] J.-D. Benamou, G. Carlier, M. Cuturi, L. Nenna, and G. Peyré. Iterative Bregman projections for regularized transportation problems. *SIAM Journal on Scientific Computing*, 37(2):A1111–A1138, 2015.
- [7] D. Bertsimas and J. N. Tsitsiklis. *Introduction to linear optimization*, volume 6. Athena Scientific Belmont, MA, 1997.
- [8] S. Borgwardt. Strongly polynomial 2-approximations of discrete Wasserstein barycenters. *arXiv preprint arXiv:1704.05491*, 2017.
- [9] S. Borgwardt and S. Patterson. On the computational complexity of finding a sparse Wasserstein barycenter. *arXiv preprint arXiv:1910.07568*, 2019.
- [10] G. Carlier, A. Oberman, and E. Oudet. Numerical methods for matching for teams and Wasserstein barycenters. *ESAIM: Mathematical Modelling and Numerical Analysis*, 49(6):1621–1642, 2015.

- [11] B. Chazelle. An optimal convex hull algorithm in any fixed dimension. *Discrete & Computational Geometry*, 10(4):377–409, 1993.
- [12] S. Chewi, T. Maunu, P. Rigollet, and A. J. Stromme. Gradient descent algorithms for Bures-Wasserstein barycenters. *arXiv preprint arXiv:2001.01700*, 2020.
- [13] M. Cuturi and A. Doucet. Fast computation of Wasserstein barycenters. In *International Conference on Machine Learning*, pages 685–693, 2014.
- [14] B. Dezső, A. Jüttner, and P. Kovács. LEMON—an open source C++ graph template library. *Electronic Notes in Theoretical Computer Science*, 264(5):23–45, 2011.
- [15] H. Edelsbrunner, J. ORourke, and R. Seidel. Constructing arrangements of lines and hyperplanes with applications. *SIAM Journal on Computing*, 15(2):341–363, 1986.
- [16] D. Ge, H. Wang, Z. Xiong, and Y. Ye. Interior-point methods strike back: Solving the Wasserstein barycenter problem. In *Advances in Neural Information Processing Systems*, pages 6891–6902, 2019.
- [17] N. Ho, X. L. Nguyen, M. Yurochkin, H. H. Bui, V. Huynh, and D. Phung. Multilevel clustering via Wasserstein means. In *International Conference on Machine Learning*, pages 1501–1509, 2017.
- [18] L. G. Khachiyan. Polynomial algorithms in linear programming. *USSR Computational Mathematics and Mathematical Physics*, 20(1):53–72, 1980.
- [19] A. Kroshnin, D. Dvinskikh, P. Dvurechensky, A. Gasnikov, N. Tupitsa, and C. Uribe. On the complexity of approximating Wasserstein barycenter. *arXiv preprint arXiv:1901.08686*, 2019.
- [20] V. M. Panaretos and Y. Zemel. Statistical aspects of Wasserstein distances. *Annual review of statistics and its application*, 6:405–431, 2019.
- [21] G. Peyré and M. Cuturi. Computational optimal transport. *Foundations and Trends in Machine Learning*, 2017.
- [22] J. Rabin, G. Peyré, J. Delon, and M. Bernot. Wasserstein barycenter and its application to texture mixing. In *International Conference on Scale Space and Variational Methods in Computer Vision*, pages 435–446. Springer, 2011.
- [23] L. Rüsendorf and L. Uckelmann. On the  $n$ -coupling problem. *Journal of Multivariate Analysis*, 81(2):242–258, 2002.
- [24] J. Solomon, F. De Goes, G. Peyré, M. Cuturi, A. Butscher, A. Nguyen, T. Du, and L. Guibas. Convolutional Wasserstein distances: Efficient optimal transportation on geometric domains. *ACM Transactions on Graphics*, 34(4):1–11, 2015.
- [25] S. Srivastava, C. Li, and D. B. Dunson. Scalable Bayes via barycenter in Wasserstein space. *The Journal of Machine Learning Research*, 19(1):312–346, 2018.
- [26] M. Staib, S. Claici, J. M. Solomon, and S. Jegelka. Parallel streaming Wasserstein barycenters. In *Advances in Neural Information Processing Systems*, pages 2647–2658, 2017.
- [27] C. Villani. *Topics in optimal transportation*. Number 58. American Mathematical Society, 2003.